Sensing Characteristics of an Optical Three-axis Tactile Sensor Mounted on a Multi-fingered Robotic Hand

Masahiro Ohka
Department of Complex Systems Science
Graduate School of Information Science, Nagoya University
Furo-cho, Chikusa-ku, Nagoya,464-8601, Japan
ohka@is.nagoya-u.ac.jp

Hiroaki Kobayashi and Yasunaga Mitsuya
Department of Electro-mechanical Enginering
Graduate School of Engineering, Nagoya University
Furo-cho, Chikusa-ku, Nagoya, 464-8603, Japan
{h_kobayashi, mitsuya}@nuem.nagoya-u.ac.jp

Abstract - **To develop a new three-axis tactile sensor for mounting on multi-fingered robotic hands, in this work we optimize sensing elements on the basis of our previous works concerning optical three-axis tactile sensors with a flat sensing surface. The present tactile sensor is based on the principle of an optical waveguide-type tactile sensor, which is composed of an acrylic hemispherical dome, a light source, an array of rubber sensing elements, and a CCD camera. The sensing element of the present tactile sensor comprises one columnar feeler and eight conical feelers. The contact areas of the conical feelers, which maintain contact with the acrylic dome, detect the three-axis force applied to the tip of the sensing element. Normal and shearing forces are then calculated from integration and centroid displacement of the gray-scale value derived from the conical feeler's contacts. To evaluate the present tactile sensor, we have conducted a series of experiments using a *y-z* stage, a rotational stage and a force gauge, and have found that although the relationship between integrated gray-scale value and normal force depends on the latitude on the hemispherical surface, it is easy to modify the sensitivity according to the latitude, and that the centroid displacement of the gray-scale value is proportional to the shearing force. Finally, to verify the present tactile sensor, we performed a series of scanning tests using a robotic manipulator equipped with the present tactile sensor to have the manipulator scan surfaces of fine abrasive papers. Results show that the obtained shearing force increased with an increase in the particle diameter of aluminium dioxide contained in the abrasive paper, and decreased with an increase in the scanning velocity of the manipulator over the abrasive paper. Because these results are consistent with tribology, we conclude that the present tactile sensor has sufficient dynamic sensing capability to detect normal and shearing forces.**

***Index Terms** – Tactile sensor, Three-axis, hemispherical, Multi-fingered hand, Optical measurement.*

I. Introduction

Tactile sensors are useful for manufacturing tasks such as assembly, disassembly, inspection and material handing [1-16]. We have previously developed an optical three-axis tactile sensor based on the principle of an optical uni-axial tactile sensor comprising an optical waveguide plate, which is made of transparent acrylic and is illuminated along its edge by a light source [13-16]. The light directed into the plate remains within it due to the total internal reflection generated, since the plate is surrounded by air having a lower refractive index than the plate. A rubber sheet featuring an array of conical feelers is placed on the plate to keep the array surface in contact with the plate. If an object contacts the back of the rubber sheet, resulting in contact pressure, the feelers collapse, and at the points where these feelers collapse, light is diffusely reflected out of the reverse surface of the plate because the rubber has a higher refractive index than the plate. The distribution of contact pressure is calculated from the bright areas viewed from the plate's reverse surface.

It is possible to improve the uni-axial tactile sensor to design the three-axis tactile sensor. In the present study on the basis of the previous studies [17-19], we developed a new sensing element for the three-axis tactile sensor, which has a columnar feeler and eight conical feelers. The eight conical feelers maintain contact with the acrylic surface while the tip of the columnar feeler touches an object. Normal and shearing forces applied to the columnar feeler tip are calculated from integrated gray-scale value and centroid displacement, respectively.

In the present study, we develop a hemispherical tactile sensor for general-purpose use of our three-axis tactile sensor, which we intend to mount on the fingertips of a multi-fingered hand. The present three-axis tactile sensor comprises an acrylic dome, a light source, an optical fiber scope, and a CCD camera. The light emitted from the light source is directed into the edge of the hemispherical acrylic dome through optical fibers. The sensing elements are arranged on the acrylic dome in a concentric configuration.

To evaluate the present tactile sensor, we conducted a series of experiments using a loading machine that consists of a *y-z* stage, a rotational stage, and a force gauge. A normal force was applied to each sensing element that lined up along the meridian of the hemisphere to examine dependence of sensing characteristics upon the latitude. The shearing force component applied to the sensing element was generated by tilting the applied force against the sensing-element axis. Finally, to verify the present tactile sensor, we performed a series of scanning tests using a robotic manipulator equipped with the present tactile sensor to have the manipulator scan surfaces of fine abrasive papers.

II. Sensing plinciple

Figure 1 shows a schematic view of the present tactile processing system to explain the sensing principle. The present tactile sensor is composed of a CCD camera, an

acrylic board, a light source, and a computer. The light emitted from the light source is directed into the optical waveguide plate. The contact phenomena are observed as image data, which are acquired by the CCD camera and are transmitted to the computer to calculate the three-axis force distribution.

The sensing element presented in this paper comprises a columnar feeler and eight conical feelers as shown in Fig. 2. The sensing elements are assembled as shown in Fig. 1 to maintain contact with the conical feelers and the acrylic board and to make the columnar feelers touch an object. The columnar feeler features a flange to fit the flange into a counter bore portion in the fixing plate to preventing the columnar feeler from horizontal displacement caused by shearing force.

If three components of force the vector F_x, F_y and F_z are applied to the tip of the columnar feeler, contact between the acrylic board and the conical feelers is measured as distribution of gray-scale values, which are transmitted to the computer. The F_x, F_y and F_z values are calculated by an integrated gray-scale value G and horizontal displacement of the centroid of gray-scale distribution $u = u_x i + u_y j$ as follows:

$$F_x = \alpha u_x, \quad (1)$$

$$F_y = \alpha u_y, \quad (2)$$

$$F_z = CG; \quad (3)$$

where i and j are orthogonal base vectors of the x- and y-axis of a Cartesian coordinate, respectively; α and C are constants estimated by calibration experiments.

III. Design of the Hemispherical Tactile Sensor

We are currently designing the multi-fingered robotic hand shown in Fig. 3 for general-purpose use in robotics. The robotic hand includes links, fingertips equipped with the three-axis tactile sensor, and micro-actuators (YR-KA01-A000, Yasukawa). Each micro-actuator consists of an AC servo-motor, a harmonic drive, and an incremental encoder, and is developed particularly for application to a multi-fingered hand.

Since the tactile sensor should be fitted to a multi-fingered hand, we are developing the fingertip to include a hemispherical three-axis tactile sensor. That is, the fingertip and the three-axis tactile sensor are united as shown in Fig. 4.

The sensing element of the tactile sensor is the same as the

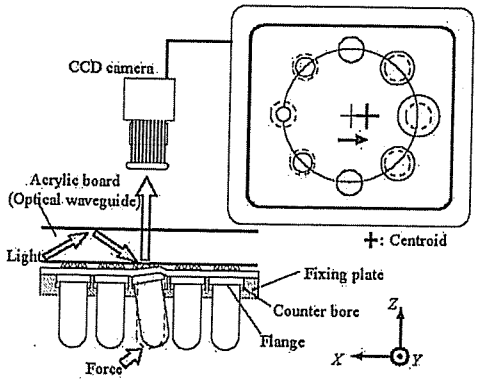

Fig. 1 Principle of the three-axis tactile sensor system

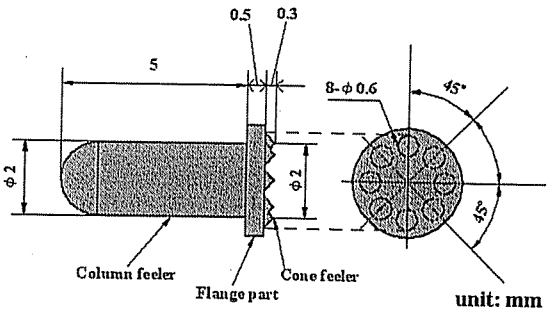

Fig. 2 Sensing element

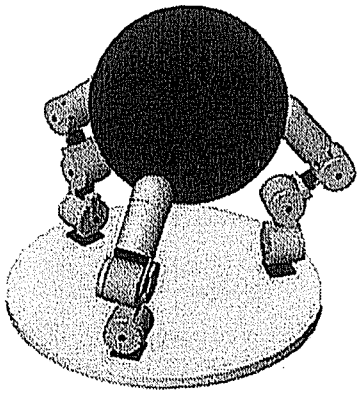

Fig. 3 A rendering of the multi-fingered hand

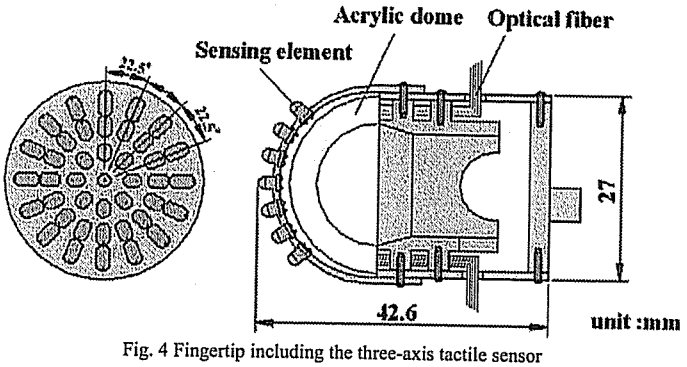

Fig. 4 Fingertip including the three-axis tactile sensor

previously described element shown in Fig. 2. The sensing elements are arranged on the acrylic dome in a concentric configuration. The acrylic dome is illuminated along its edge through the optical fibers connected to the light source. Image data of bright spots caused by the feelers collapse is retrieved by an optical fiber-scope connected to the CCD camera.

IV. Experimental Conditions

A. Experimental apparatus

We developed a loading machine that includes an x-stage, a z-stage, a rotary stage, and a force gauge (FGC-0.2B, NIDEC-SHIMPO Co.) to detect sensing characteristics of normal force and shearing force. The force gauge has a probe to accept force and can detect force in the range of from 0 to 2 N with a force resolution of 0.001 N. The positioning precisions of the y-stage, the z-stage, and the rotary stage are 0.001 mm, 0.1 mm and 0.1 °, respectively.

B. Normal force sensing

Because the present tactile sensor can detect not only normal force but also shearing force, we should confirm the sensing capability for both of these forces. In normal-force testing, by applying a normal force to the tip of a sensing element using the z-stage after rotating the attitude of the tactile sensor, it is easy to test the specified sensing element using the rotary stage. Since the rotary stage's centre of rotation coincides with the centre of the present tactile sensor's hemispherical dome, it is easy to test any sensing elements aligned along the hemisphere's meridian.

C. Shearing force sensing

When we want to generate the shearing-force component, both the rotary stage and the x-stage are operated to specify the force direction and sensing element. At first, the rotary stage is operated to specify the force direction, ϕ. Then, the x-stage is tuned to the applied tilted force at the tip of the specified sensing element. Figure 6 exemplifies that the sensing element located on the parietal region can be assigned according to the abovementioned procedure. After that, a force is loaded onto the tip of the sensing element using the z-stage. Regarding the manner of loading, since the force direction does not coincide with the axis of the sensing element, slippage between the probe and the tip of sensing element occurs. Therefore, a spherical concave portion is made on the probe surface to mate the concave portion with the hemispherical tip of the tactile element.

D. Surface scanning test

Because the development of the robotic fingers is continued, we used a surface-scanning system comprised of a robotic manipulator (KS-V20, Matsushita, Co.) equipped with the present tactile sensor and the tactile data processing system [18] to evaluate dynamic sensing characteristics of the present tactile sensor. The image processing board (Himawari PSI/S, Library Co.) in the computer can process the image data from the present tactile sensor within 1/30 sec at each data sampling.

We performed surface-roughness estimation tests using the abovementioned surface scanning system. The robotic manipulator rubbed a fine abrasive paper plastered onto an x-y-z stage with the sensing surface of the present tactile sensor, scanning the abrasive paper. We adopted three types of abrasive paper (Wrapping film, 3M) including 5-, 15- and 30-μm grade paper, and also Teflon film, as specimens. The robotic manipulator scanned these specimens at four different scanning speeds (100, 200, 300 and 400 mm/s) to evaluate the effect of velocity on the shearing force.

V. Experimental Results and Discussion

A. Normal force sensing

To evaluate the present hemispherical tactile sensor, we conducted a series of experiments using the loading machine. Figure 7 shows variation in the integrated gray-scale value caused by increase of the normal force. As Fig. 7 indicates, in

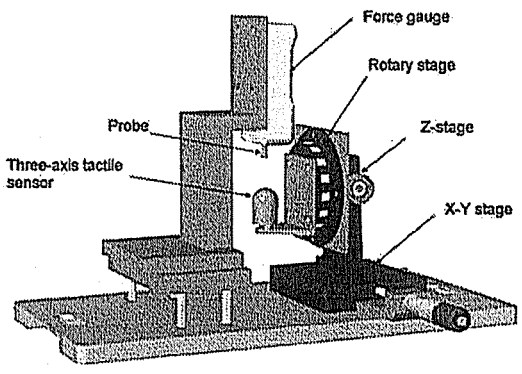

Fig. 5 Loading machine

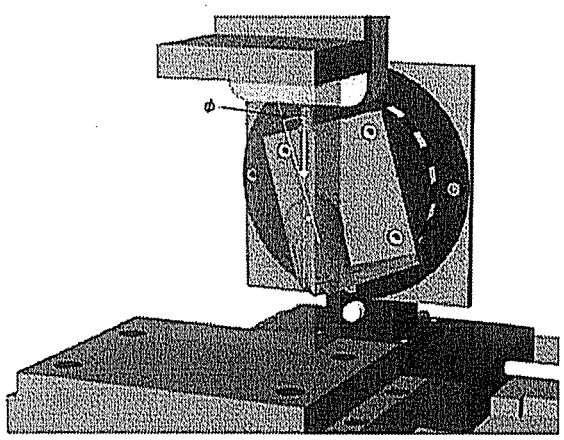

Fig. 6 Generation of shearing force component

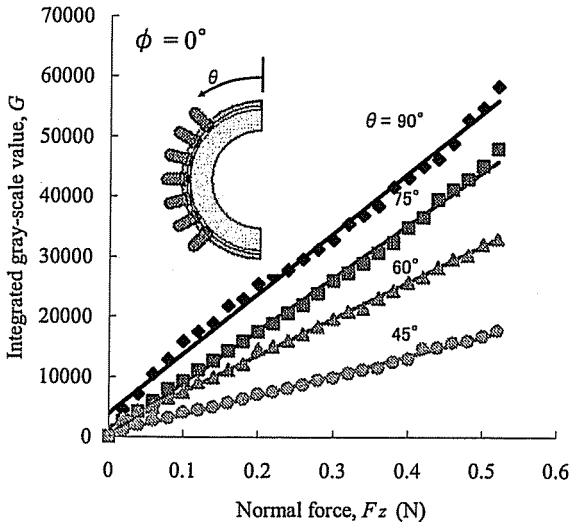

Fig. 7 Experimental results approximated by the least-squares method

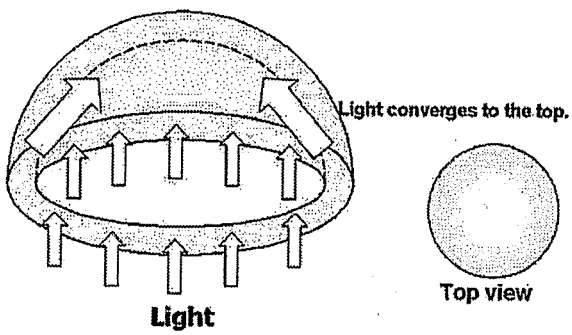

Fig. 8 Principle of obtaining different sensitivities depending on the latitude

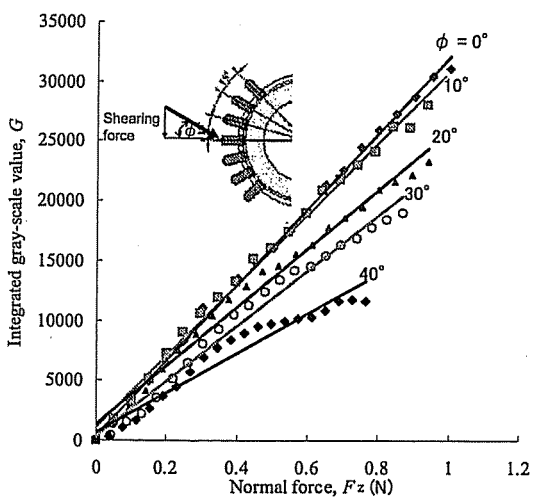

Fig. 9 Relationships between integrated gray-scale value and normal-force component under several conditions of ϕ

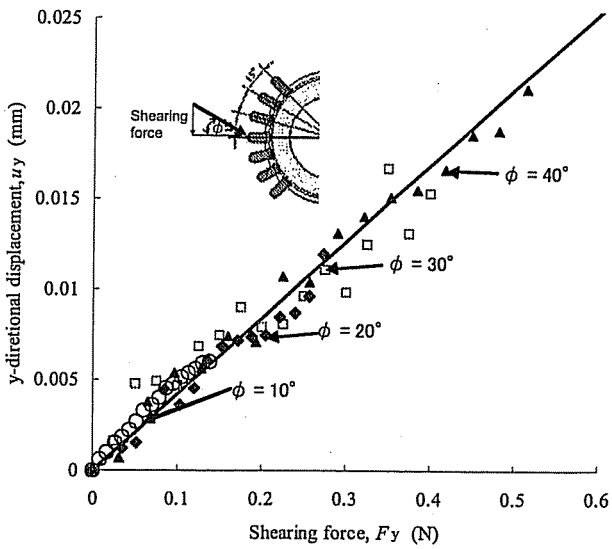

Fig. 10 Variations in centroid of contact area

spite of the latitude, θ, the relationships between the integrated gray-scale value and normal force show good linearity because values of the square of the correlation coefficient, R^2, fall within the range of 0.992 to 0.998. Note, however, that the gradient of each solid line increases with an increase in θ; that is, the sensitivity depends upon the latitude on the hemisphere.

Dome brightness is inhomogeneous because the edge of the dome is illuminated and light converges on the parietal region of the dome, as Fig. 8 shows. The brightness is represented as a function of the latitude, θ, and since the sensitivity is uniquely determined by the latitude, it is easy to modify the sensitivity according to θ

B. Shearing force sensing

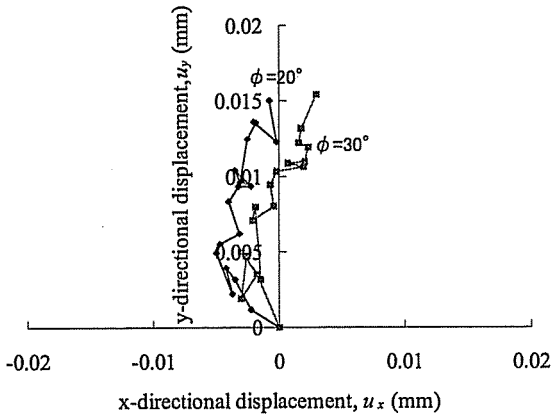

Fig. 11 Trajectory of centroid of contact area in the x-y plane

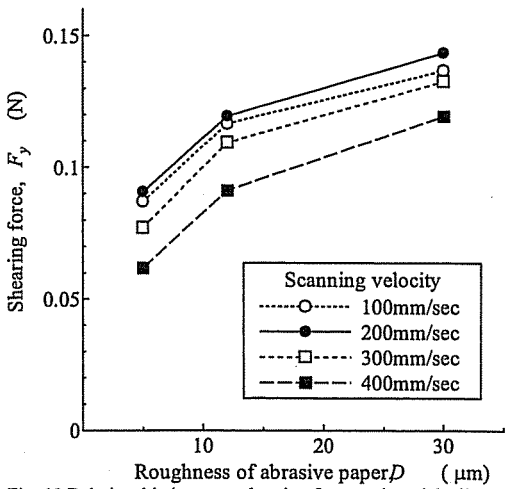

Fig. 12 Relationship between shearing force and particle diameter

When force is applied to the tip of the sensing element located in the parietal region under several ϕ s, relationships between the integrated gray-scale value and normal-force component are obtained as shown in Fig. 9. The relationships show good linearity as well because values of R^2 fall within range of 0.945 to 0.998. Although the gradient should take a constant if the normal force component is calculated by Eq. (3), it depends on the force direction, ϕ.

Next, Fig. 10 shows variations in centroid displacement of the contact areas. Centroid displacement grows with increases in the shearing force component. In contrast with the variation in the integrated gray-scale value, however, the centroid movement scatters around the approximated single straight line.

The scattering seems to be caused by a slight vibration induced by manual operation of the z-stage. The centroid displacement moves two-dimensionally inside an x-y tangential plane set on the top of the hemispherical dome. As Fig. 11 shows, the x-directional displacement occurs despite the lack of an x-directional force component; the trajectory scatters due to the vibration. In future work, we will attempt to improve the loading machine in order to apply precise y-directional force to the sensing element by using a precise motor-driven z-stage. After that, we will obtain a method to modify the relationships shown in Figs. 9 and 10.

C. Scanning test

To evaluate the effect of grain-size on the shearing force, in Fig. 12 we show the relationships between the shearing force and the abrasive grain diameter. It is evident from this figure that the shearing force increases with an increase in the diameter of the abrasive grains, meaning the shearing force can be used to discriminate between the three types of abrasive paper.

Next, Fig. 13 shows the relationship between the shearing force and the scanning velocity, revealing the

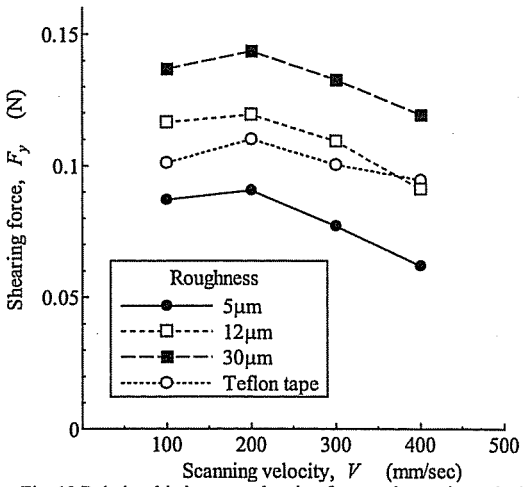

Fig. 13 Relationship between shearing force and scanning velocity

scanning speed's effect on the shearing force. Variations in the normal force decrease with an increase in scanning velocity over the abrasive papers, as shown in this figure, whereas the shearing force remains almost constant in the case of Teflon.

As mentioned above, the tribological characteristic of the abrasive paper does not conform to Coulomb's law because the tangential force depends on the scanning velocity. In the case of Teflon, however, the tangential force does not depend on the scanning velocity, thus its tribological characteristic conform to Coulomb's law. These results are plausible because grinding between the tip of the conical feeler and the abrasive grains occurs in the case of the abrasive paper,

decreasing the tangential force as a result of increasing the scanning velocity, according to the cutting theory. Therefore, the present tactile sensor can measure dynamic behaviours with respect to tribology and the cutting theory.

VI. Conclusion

In order to produce a new three-axis tactile sensor for mounting on multi-fingered robotic hands, we developed a new three-axis tactile sensor based on the principle of an optical waveguide-type tactile sensor comprising an acrylic hemispherical dome, a light source, an array of rubber sensing elements, and a CCD camera. The sensing element of the present tactile sensor includes one columnar feeler and eight conical feelers. A three-axis force applied to the tip of the sensing element is detected by contact areas of the conical feelers, which maintain contact with the acrylic dome. Normal and shearing forces are calculated from integration and centroid displacement of the gray-scale value derived from the conical feeler's contacts.

To evaluate the present tactile sensor, we conducted a series of experiments using a *y-z* stage, a rotational stage, and a force gauge. Although the relationship between the integrated gray-scale value and normal force depended on the latitude on the hemispherical surface, it was easy to modify the sensitivity according to the latitude. Results indicted that centroid displacement of the gray-scale value was proportional to the shearing force. The tactile sensor was mounted on a robotic manipulator to evaluate its practical use. The robotic manipulator rubbed fine abrasive papers and a Teflon film with the sensing surface of the present tactile sensor. Findings revealed that the present tactile sensor can measure the difference of tribological behaviours between abrasive paper and a Teflon surface. Therefore, we conclude that the present tactile sensor has sufficient dynamic sensing capability to detect normal and shearing forces.

References

[1] Raibert, H.M. and Tanner, J.E., Design and Implementation of a VSLI Tactile Sensing Computer, Int. J. Robotics Res., Vol. 1-3(1982), pp. 3-18.

[2] Hackwood, S., Beni, G., Hornak, L. A., Wolfe, R. and Nelson, Torque-Sensitive Tactile Array for Robotics, Int. J. Robotics Research, Vol. 2-2 (1983), pp. 46-50.

[3] Dario, P., Rossi, D.D., Domenci, C. and Francesconi, R., Ferroelectric Polymer Tactile Sensors with Anthopomorphic Features, Proc. 1984 IEEE Int. Conf. On Robotics and Automation, (1984), pp. 332-340.

[4] Novak, J. L., Initial Design and Analysis of a Capacitive Sensor for Shear and Normal Force Measurement, Proc. of 1989 IEEE Int. Conf. On Robotic and Automation, (1989), pp. 137-145.

[5] Hakozaki, M. and Shinoda, H., Digital Tactile Sensing Elements Communicating Through Conductive Skin Layers, Proc. of 2002 IEEE Int. Conf. On Robotics and Automation, 2002, pp. 3813-3817.

[6] Yamada, Y. and Cutkosky, R., Tactile Sensor with 3-Axis Force and Vibration Sensing Function and Its Application to Detect Rotational Slip, Proc. of 1994 IEEE Int. Conf. On Robotics and Automation, 1994, pp. 3550-3557.

[7] Nicholls, H.R.& Lee, M.H., A Survey of Robot Tactile Sensing Technology, Int. J. Robotics Res., Vol. 8-3, (1989), pp. 3-30.

[8] Bicchi, A., Salisbury, J. K. and Dario, P., Augmentation of Grasp Robustness Using Intrinsic Tactile Sensing, Proc. of 1989 IEEE Int. Conf. On Robotics and Automation, 1989, pp. 303-307.

[9] Howe, R. D.. and Cutkosky M. R., Dynamic Tactile Sensing: Perception of Fine Surface Features with Stress Rate Sensing, IEEE Trans on Robotics and Automation, Vol. 9, No. 2, (1993), pp. 140-151.

[10] Ohka, M. et al., Tactile Expert System Using a Parallel-fingered Hand Fitted with Three-axis Tactile Sensors, JSME Int. J., Series C, Vol. 37, No. 1, 1994, pp. 138-146.

[11] Takeuchi, S., Ohka, M. and Mitsuya, Y., Tactile Recognition Using Fuzzy Production Rules and Fuzzy Relations for Processing Image Data from Three-dimensional Tactile Sensors Mounted on a Robot Hand, *Proc. of the Asian Control Conf.*, Vol. 3, 1994, pp. 631-634.

[12] B. Borovac, L. Nagy and M. Sabli, Contact Tasks Realization by sensing Contact Forces, Theory and Practice of Robots and Manipulators (Proc. of 11th CISM-IFToNN Symposium), Springer Wien New York, (1996), pp. 381-388.

[13] H. Mott, M. H. Lee, and H. R. Nicholls, "An Experimental Very High Resolution Tactile Sensor Array", in Proc. 4th Int. Conf. On Robot Vision and Sensory Control, pp. 241-250, 1984.

[14] K. Tanie, K. Komoriya, M. Kaneko, S. Tachi, and A. Fujiwara, "A High Resolution Tactile Sensor Array", Robot Sensors Vol. 2: Tactile and Non-Vision, Kempston, UK: IFS (Pubs), pp. 189-198, 1986.

[15] H. R. Nicholls, "Tactile Sensing Using an Optical Transduction Method", Traditional and Non-traditional Robot Sensors (Edited by T. C. Henderson), Springer-Verlag, pp. 83-99, 1990.

[16] H. Maekawa, K. Tanie, K. Komoriya, M. Kaneko, C. Horiguchi, and T. Sugawara," Development of Finger-shaped Tactile Sensor and Its Evaluation by Active Touch", in Proc. of the 1992 IEEE Int. Conf. on Robotics and Automation, pp. 1327-1334, 1992.

[17] M. Ohka, Y. Mitsuya, S. Takeuchi, H. Ishihara, and O. Kamekawa, "A Three-axis Optical Tactile Sensor (FEM Contact Analyses and Sensing Experiments Using a Large-sized Tactile Sensor)", in Proc. of the 1995 IEEE Int. Conf. on Robotics and Automation, pp. 817-824, 1995.

[18] M. Ohka, Y. Mitsuya, Y. Matsunaga, and S. Takeuchi, "Sensing Characteristics of an Optical Three-axis Tactile Sensor Under Combined Loading", Robotica, vol. 22, pp. 213-221, 2004.

[19] M. Ohka, Y. Mitsuya, I. Higashioka and H. Kabeshita, "An experimental optical three-axis tactile sensor for micro-robots", Robotica, (to be published)